Nanoparticles' Role in Advancing Agriculture: A comparative study of green and chemically synthesized nanoparticles and their influence on root and shoot morphology of Sunflower

N Pruthviraj
University of Agricultural Sciences
K N Geetha
University of Agricultural Sciences
G N Anil Kumar
MSRIT: Ramaiah Institute of Technology
D L Shruthi
Sai Vidya Institute of Technology
A G Shankar
College of Agriculture
S S Prakash
College of Agriculture
Shankarappa Sridhara
University of Agricultural and Horticultural Sciences
A V Raghu (gsraghu2003@yahoo.co.in)
BLDE Deemed to be University - Smt Bangaramma Sajjan Campus: BLDE Deemed to be University
https://orcid.org/0000-0003-0299-7409

Research Article

Keywords: h-boron nitride, Sulphur, root length, and germination per cent, UV-Visible

Posted Date: October 12th, 2023

DOI: https://doi.org/10.21203/rs.3.rs-3361246/v1

Nanoparticles' Role in Advancing Agriculture: A comparative study of green and chemically synthesized nanoparticles and their influence on root and shoot morphology of Sunflower

Abstract

The eco-friendly synthesis approach was employed to create nanoparticles by harnessing the inherent properties of natural sources. *Cassia fistula* leaf extract was utilized for boron nitride production, while *Simarouba glauca* was employed for sulphur nanoparticles. The nanoparticles' characterization involved identifying functional groups through various analytical techniques, including FT-IR, Raman spectroscopy, and UV-visible spectroscopy. Furthermore, ab initio studies were conducted to uncover the electronic properties of the boron nitride and sulphur nanostructures. The structural analysis of the boron nitride nanoparticles revealed a hexagonal configuration through Powder X-ray diffraction tests, while the sulphur nanoparticles exhibited an orthorhombic structure. In-depth examinations utilizing scanning electron microscopy and transmission electron microscopy showcased particle sizes below 100 nm. In a laboratory experiment, sunflower seeds treated with 1500 ppm green-synthesized nano boron nitride demonstrated remarkable root morphology and achieved the highest germination percentage of an impressive 98.2%, surpassing other concentration levels. Importantly, the eco-friendly synthesized nanoparticles displayed greater efficacy when compared to both chemically synthesized nanoparticles and conventional fertilizers.

Key Message:

Keywords: *h*-boron nitride, Sulphur, root length, and germination per cent, UV-Visible,

1. Introduction

Amidst the intricate fabric of sunflower cultivation, it's *vital* to emphasize the pivotal roles of major and micronutrients. While the former garners rightful attention, the latter group, encompassing zinc, iron, manganese, copper, boron, and zinc, profoundly contributes to sunflower physiology [Wanga et al. 2018; Pruthviraj and Chandrashekara 2021b]. These micronutrients intricately interlace with enzymatic functions, serving as catalysts in reactions that orchestrate a symphony of plant activities [Suresh et al. 2015]. Their significance reaches beyond their minimal quantities, extending from respiration to chlorophyll formation, photosynthesis, energy systems, and the synthesis of proteins, oils, tannins, and phenolic compounds[Prasad et al. 2012; Ouvrard et al. 1996; Du et al. 2018].

Boron, a micronutrient essential for crops, stands out as a contributor. Its influence is profound, yet a delicate balance is required as high concentrations can be detrimental [Aarti et al. 2019]. In the realm of sunflowers, boron aids in flowering, pollen germination, tube growth, and seed development. Particularly vital for this crop due to its sensitivity to boron deficiency, its application amplifies growth, enhances pollen characteristics, and facilitates vital compound translocation, culminating in increased productivity [Chen et al. 2018; Khairan et al. 2019].

Sulphur, a versatile non-metallic element, holds essential status in the global economy, found in fertilizers and various products [Chaudhari and Paria 2010]. Its shortage in Indian soils underscores its importance. Sulphur's impact on photosynthesis and carbon assimilation is a significant aspect contributing to oil content. It fosters chlorophyll production, driving enhanced photosynthesis and increased carbon compounds, which translate into heightened oil synthesis. Research highlights sulphur's influence on oil accumulation across diverse crops [Awwad et al. 2015; Li et al. 2008; Maiti and Giri 2003].

In the realm of modern agriculture, the pursuit of sustainable practices fostering higher yields has spurred innovative techniques. Nanoparticles, a promising avenue, offer solutions for enhanced crop growth while minimizing resources and environmental impact [Marschner et al. 1986]. Nanotechnology's integration into agriculture spans domains such as nano-pesticides, nano-herbicides, nano-fertilizers, and nano-hydrogels [Chitdeshwari and Poongothai 2003; Medina-Parez et al. 2018]. Of particular interest is the application of nanoparticles to seeds, bolstering defences against pests and elevating germination percentages in various crops. Sunflower cultivation, for instance, benefits from nano boron nitride seed treatments that enhance germination rates and seedling establishment [Prasad et al. 2012]. Nano sulphur-treated seeds exhibit robust root growth parameters, especially under water-stressed conditions [Nida et al. 2016].

Considering the landscape of nano fertilizer implementation, a significant distinction emerges. Nano fertilizers synthesized through green routes outperform their commercially synthesized counterparts, aligning with sustainable practices [Suleiman et al. 2015; Maryam et al. 2022; El-Bialybe et al. 2017; Faten et al. 2018]. Their capacity to amplify seed germination through heightened metabolic activity resonates with the call for eco-friendly agricultural approaches, reducing the need for bulk fertilizers [Geetha et al. 2018; Hemantharanjan et al. 2018].

In this experiment, different leaf extracts were used as reducing and stabilizing materials for the synthesis of nanoparticles. Five weed species (*Parthenium hysterophorus, Calotropis gigantea, Tridax procumbens, Alternanthera sessilis and Cynodon dactylon*) and five tree species (*Cassia fistula, Pongamia pinnata, Azadirachta indica, Simarouba glauca and Ficus benghalensis*) were used in the synthesis process. Among these weeds and tree species, *Cassia fistula* contains a higher amount of phenolics and is considered a good reducing and stabilizing agent [Joshi and Joshi 2002]. If the leaf extract contains a higher amount of phenolics, it reduces the particles to nano-size [Russell and Mussa 1977; Rahimi and Bussler 1973]. To synthesize nano boron nitride, *Cassia fistula* and for nano sulphur *Simarouba glauca* leaf extractant was used. In the present study, green-synthesized boron nitride and sulphur nanoparticles were characterized using different spectroscopic techniques, such as Powder X-ray diffraction (PXRD), UV – VIS spectrophotometry, particle size analysis, Scanning Electron Microscope (SEM), Transmission Electron Microscope (TEM), Atomic force microscope (AFM), FTIR, and Raman spectroscopy, to identify the size, shape, morphology, and other properties of nanoparticles.

Numerous researchers have successfully synthesized nano boron nitride via the green synthesis approach [Aarti et al. 2019; Chen et al. 2018; Geetha et al. 2018; Weon et al. 2011], alongside the green synthesis of nano sulfur [Suleiman et al. 2015; Kozegaran and Farhadi 2017]. It's worth noting that variations exist not only in the plant extractants employed for the synthesis but also in the geographical availability of the same plant species worldwide. Certain species are confined to specific regions or countries. In our specific context, we embarked on an exploration involving five weed species and five tree species, with the objective of identifying plant extracts rich in phenolic content capable of facilitating the transformation of particles into their nano counterparts.

The scientific community has indeed recognized the significance of utilizing green-synthesized nanoparticles for foliar application in diverse research endeavours. However, the utilization of nanoparticles for seed treatment has remained constrained, and a discernible knowledge gap exists pertaining to their influence on root germination and ensuing root growth. Motivated by these pertinent gaps, our current study endeavours to holistically evaluate the impact of nanoparticles on both shoot and root development, specifically within the context of sunflower cultivation. Consequently, this research undertakes a comprehensive characterization of nanoparticles synthesized through diverse methodologies, shedding light on the distinct attributes of each, and underscoring their relative effectiveness.

This study serves as a vital bridge between past achievements and emerging inquiries within the realm of nanotechnology. By juxtaposing green and chemical synthesis pathways, it strives to unravel the nuances that underscore their respective contributions. This journey encompasses the exploration of nanoparticle efficacy and opens avenues for fostering sustainable agricultural practices through the optimal use of nanoparticles.

2. Experimental procedure

2.1 *Experimental procedure for the extraction of Cassia fistula and Simarouba glauca leaf extractant and green synthesis of nano boron nitride (nBN) and nano sulphur (nS)*

Leaf extractant: Fresh leaves of both *Cassia fistula* and *Simarouba glauca* were procured from a university campus. They underwent cleaning under tap water to eliminate debris, followed by several washes with distilled water. After being air-dried for a duration of 4 weeks, the leaves were ground into a fine powder utilizing a mixer grinder, subsequently sieved through a 20-mesh sieve, and stored appropriately. Subsequently, 20 g of this powdered material from each species was combined with 400 mL of deionized water in separate 500 mL beakers. These mixtures were then subjected to heating at 65°C for 30 minutes for *Cassia fistula* and 60°C for 20 min for *Simarouba glauca*. The ensuing leaf extracts were isolated through a process of double filtration and centrifugation, and subsequently preserved at room temperature, maintaining separate storage for each species.

Nano boron nitride: In a beaker, boron nitride (9.5 g) was added to boiling water at 125°C with continuous stirring. *Cassia fistula* leaf extract (45 mL) was then introduced into the solution while maintaining stirring for 10 min. The heating procedure was sustained alongside consistent stirring for a duration of 90 min. Following this, the stirring was left uninterrupted for 3 hr, and subsequently, the supernatant was gathered and subjected to centrifugation at 1500 rpm for 30 minutes. Post-centrifugation, the particles underwent freeze-drying to yield the Nanosheets.

Nano Sulphur: In a beaker, sodium thiosulfate pentahydrate ($Na_2S_2O_3.5H_2O$; 12 g) was added to boiling water (125°C) while maintaining continuous stirring. After 20 minutes, 100 mL of *Simarouba glauca* leaf extract was introduced, and the mixture was stirred continuously for 5 minutes at room temperature. Subsequently, 5-6 drops of citric acid (lemon juice) were added drop by drop with stirring. This initiated a reaction resulting in the formation of sulfur dioxide, sulfur, and water. As sulfur dioxide is a soluble gas, it completely dissolved in the aqueous solution. The precipitated sulfur appeared as a pale yellow substance. Following this, the obtained material underwent centrifugation at 1200 rpm for 5 min, leading to the separation of the supernatant, which was subsequently discarded. The resulting yellow precipitate was washed repeatedly with sterile distilled water and then subjected to a muffle furnace at 400°C for 30 minutes. This process yielded a fine yellow material known as sulfur nanoparticles. The final product was securely stored in an airtight container for future use.

Commercially available/chemically synthesis of nano boron nitride and nano Sulphur:

Nano boron nitride was synthesized by following the procedure of [Dongping et al. 2008; Aarti et al. 2019], similarly for sulphur [Suleiman et al. 2015; Kouzegaran and Farhadi 2017].

2.5 LABORATORY STUDIES

A laboratory study was conducted to analyze the germination percentage, root morphology (using a root scanner), seedling vigour, and other parameters related to the seedling development of sunflower seeds. This analysis involved the utilization of different forms and concentrations of nBN (nano boron nitride) and nS (nano sulphur) fertilizers.

Germination test: In accordance with International seed testing association (Anonymous 2011) regulations, the seed germination test for the sunflower hybrid KBSH-53 (*Helianthus annuus* L.) was conducted using non-toxic germination paper as the medium. Sunflower seeds were exposed to varying nBN and nS concentrations, including 250, 500, 750, 1000, 2000, and 3000 ppm of green-synthesized particles (GsP) and commercially available particles (CP) for nBN, nS, and the control. Each treatment utilized 100 seeds, with triplicate examinations. The seeds were placed between paper towels, enclosed, and positioned within a seed germinator set at a temperature of 25°C and relative humidity of 95 percent. Germination percentages were calculated based on normal, deformed, and non-germinated seedlings, as well as diseased seeds, as per the procedure described in [Anonymous 2011].

Significant enhancements in seedling development parameters were observed during the initial laboratory trials within the range of 1000 ppm to 2000 ppm for nBN and 500 ppm to 750 ppm for nS. In the subsequent series of experiments, concentrations of 550, 600, 650, 700, 750, and 800 ppm for both commercially available and green-synthesized nS were employed. Similarly, concentrations of 1000, 1250, 1500, 1750, 2000, and 2250 ppm for commercially available and green-synthesized nBN particles, along with the control, were tested. Each treatment was replicated three times in the laboratory, with observations recorded for normal, abnormal, dead, and diseased seeds. Germination percentages were noted twice, at 5 days and 10 days after sowing

Germination percentage

The number of germinated seedlings for each treatment was recorded visually. The germination percentage was estimated using the following formula:

$$\text{Germination (\%)} = \frac{\text{No. of germinated seeds}}{\text{Total No. of seeds kept for germination}} \times 100$$

Seedling vigour index I= Germination (%) × total seedling length (cm)

Seedling vigour index II= Germination (%) × seedling dry weight (mg)

Mean days of germination ($\bar{t}$)

The mean number of days required for total germination for a particular treatment was calculated using the following formula [Edwards et al. 1932]:

$$\bar{t} = \frac{N_1T_1 + N_2T_2 + \cdots N_kT_k}{N_1 + N_2 + \cdots N_k}$$

where, $\bar{t}$ = time in days starting from day '0'

N= is the number of seeds completing germination on the day 't'.

Co-efficient of velocity of germination (CVG)

The coefficient velocity of germination as influenced by different treatments was calculated using the following formula [Edwards et al. 1932]:

$$CVG = \frac{N_1 + N_2 + \cdots N_k}{N_1T_1 + N_2T_2 + \cdots N_kT_k \ \ N_1} \times 100$$

Where, 'N' is the number of germinating seeds within the consecutive intervals of time 'T' and 'T' is the time between the beginning of the test and the end of the particular intervals of measurement.

Mean daily germination (MDG)

The final germination percentage at the end of the test divided by the number of days was expressed as the mean daily germination, as described by [Edwards et al. 1932]:

Root scanner:

The WinRHIZO root scanner from Regent Instruments, Canada, is an image analysis system developed for root measurement in several forms, including average root diameter, root volume, root length volume (average root diameter plus root length), and forks. Washed roots of sunflower seedlings from the two sets of laboratory treatments were interactively analyzed using a WinRHIZO root scanner.

Statistical analysis and interpretation of data

The data gathered from studies at various phenological phases were statistically analyzed. In the laboratory experiment, the level of significance in the 'F' and ‘t' tests was 5% (P=0.05) or (F- test *) and 1% (P=0.01) or (F- test **). Wherever the F-test was determined to be significant for comparing the treatment means, an appropriate critical difference (CD) was calculated. Otherwise, NS was used to denote the CD values.

3. Result and Discussion

3.1 Characterization of nanoparticles

3.1.1 Powder X-ray diffraction (PXRD)

Fig. 1(a) and **Fig. 1(b)** show the refined PXRD patterns obtained after Rietveld refinement of boron nitride and sulphur nanoparticles. All strident diffraction peaks are in indenture with JCPDS card 00-034-0421 for boron nitride and JCPDS card 000-074-1465 for sulphur. Boron Nitride has a hexagonal structure with phase purity in the P63/mmc space group. The Sulphur nanoparticles confirm Orthorhombic structure with a space group of *Fddd*. No impurity peaks were observed, confirming the high crystallinity.

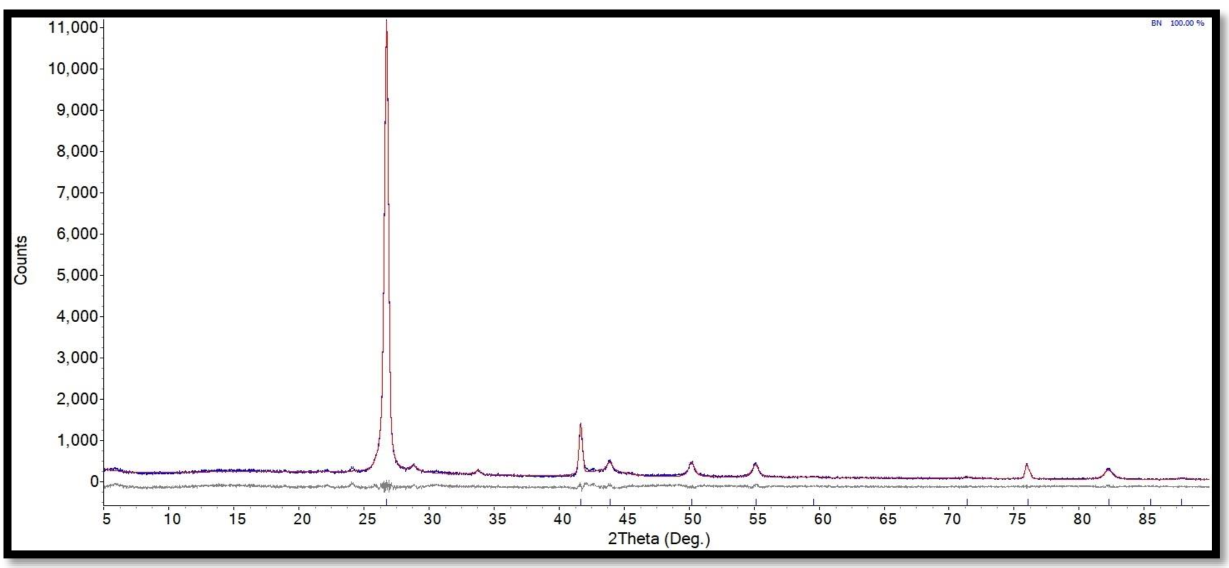

Fig. 1(a) PXRD Rietveld refinement pattern of boron nitride nanoparticle.

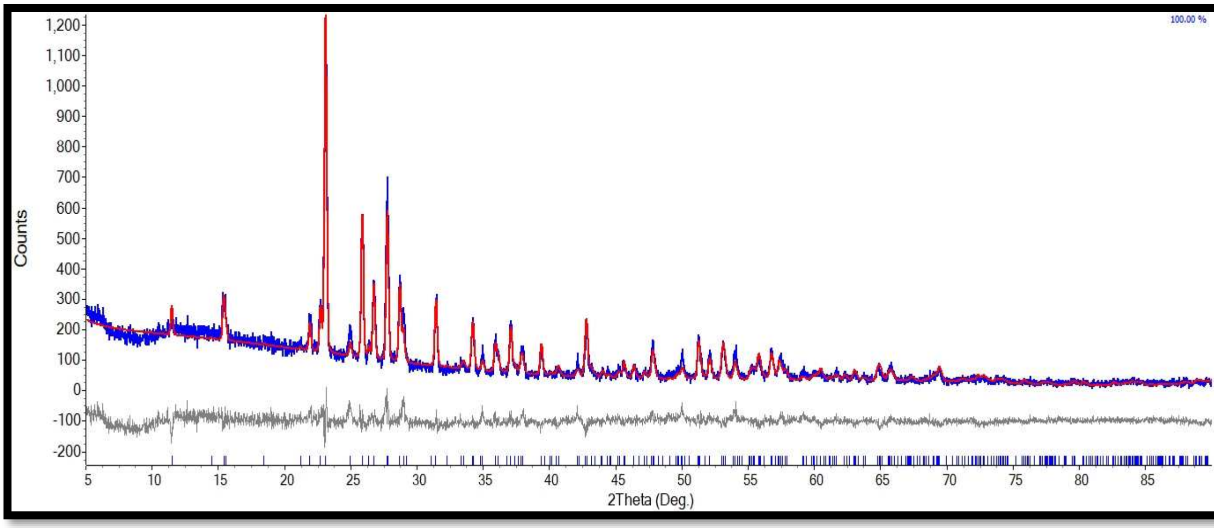

Fig. 1(b) PXRD Rietveld refinement patterns of sulphur nanoparticle.

Using the Debye Scherrer reckoning, the typical crystallite size of the ready sample was considered as follows:

$$D = \frac{k\lambda}{\beta cos\theta} \qquad \ldots\ldots\ldots\ldots\ldots\ldots\ldots\ldots\ldots\ldots\ldots\ldots\ldots (1)$$

where, β is the full width at half maximum, θ is the glancing angle, D is the average crystal size, λ = 1.5418 Å is the wavelength of the X-rays used, and k = 0.89 is the shape factor [Anilkumar and Shruthi 2021]. The average crystallite size was institute to be nearly 38.9 nm for boron nitride and 65 nm for sulphur nanoparticles.

BN crystallized in a hexagonal crystal system with the space group P63/mmc. The two dimensional structure consists of two BN sheets oriented in the Z direction. The B^{3+} ion is bonded to three equivalent N^{3-} atoms in a trigonal planar geometry, while N^{3-} is bonded to three equivalent B^{3+} atoms in trigonal planar geometry. The structure of sulphur consists of sixteen zero-dimensional Sulpur clusters in the unit cell with four inequivalent sites. At each site, sulphur was bonded to two S atoms in a water-like geometry. **Table 1** shows the refinement outcomes for all strictures. In the hexagonal structure, the atomic sites of B (4b; 0, 0.25, 0.625) and N (4a; 0, 0.25, 0.125) were refined using the pseudo-Voigt function to model the peak profiles with six coefficient polynomials to designate the background.

Table 1: The Refinement results for all parameters

Phase	**Boron Nitride**				**Sulphur**	
Crystal System	*Hexagonal*				*Orthorhombic*	
Space group	*P63/mmc (194)*				*Fddd*	
Lattice Parameters(Å)						
a	2.500(2)				10.461(8)	
b	2.500(2)				12.864(4)	
c	6.662(4)				24.484(7)	
α, β, γ	90,90,120				90,90,90	
Cell volume (Å^3)	36.086(2)				3295.4	
Atomic Coordinates						
Atoms	X	y	z	B	Occ.	Np
B	0.333	0.666	0.250	1.0	1.0	6
N	0.333	0.666	0.750	1.0	1.0	6
S1	-0.017	0.083	0.072	1.0	1.0	32

S2	-0.094	0.161	0.200	1.0	1.0	32
S3	-0.167	0.105	0.125	1.0	1.0	32
S4	-0.094	0.028	0.250	1.0	1.0	32
Refined parameters						
R_{exp}	R_{wp}	R_p	GooF	Crystallite size (nm)	Density (g/cm^3)	Strain
6.36	9.34	6.72	1.47	38.9	6.852	0.00108
10.28	13.97	10.69	1.36	48.6	2.068	0.00016

3.1.2 Computational details

Periodic compactness functional theory designs were performed in the CRYSTAL17 code using PBE hybrid functionals [Deane and Smith 2018; Shruthi et al. 2020]. The Monk horst-pack mesh has a shrinking factor of six in the reciprocal space of the Brillouin zone of the primitive cell. The thresholds controlling the accuracy were set to 10^{-7} for ITOL1–ITOL4 and 10^{-14} for ITOL5. For all geometry optimizations, the self-consistent field convergence (SCF) on the energy was set to 10^{-8}hartree. In **Fig. 2(a)** and **Fig. 2(b),** the electron density (ρ) distributions (a) and (c), deformation density ($\Delta\rho$), and (b) and (d) for BN resultant from the crystalline density, respectively. The deformation density is exhibited in bold for null values, dense lines for positive values, and dotted lines for negative values. Positive values of deformation density show charge accumulation, while negative values represent electron flow in the case of interacting atoms.

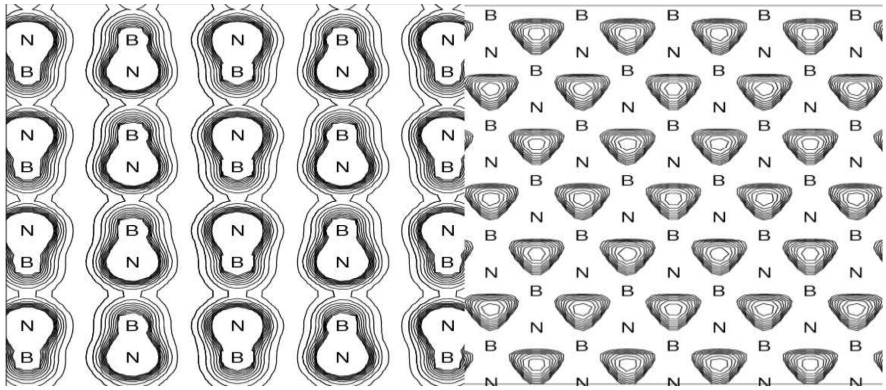

Fig. 2(a) Electron density (ρ) deformation density (Δρ) maps of nano boron nitride.

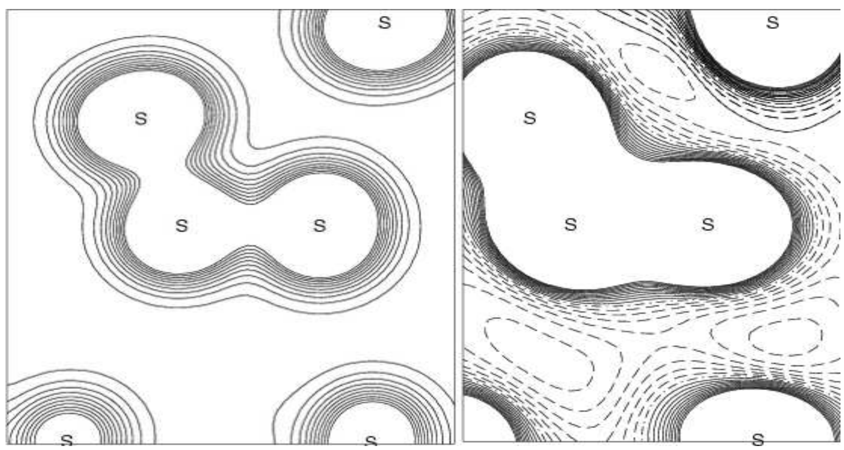

Fig. 2(b) Electron density (ρ) deformation density (Δρ) maps of nano Sulphur

3.1.3 Scanning electron microscope

SEM was employed to measure the size of the nanoparticle, as shown in **Fig. 3a** for boron nitride and **Fig. 3b** for sulphur nanoparticles. The principle of SEM is magnification of the targeted object. Hence, these approaches provide the exact sizes of the particles synthesized using the green synthesis approach. The SEM images show that the green-synthesized boron nitride and sulphur nanoparticle samples were less than 100 nm in size and were homogenously dispersed. The larger particles were due to the aggregation of the smaller particles in the SEM measurements.

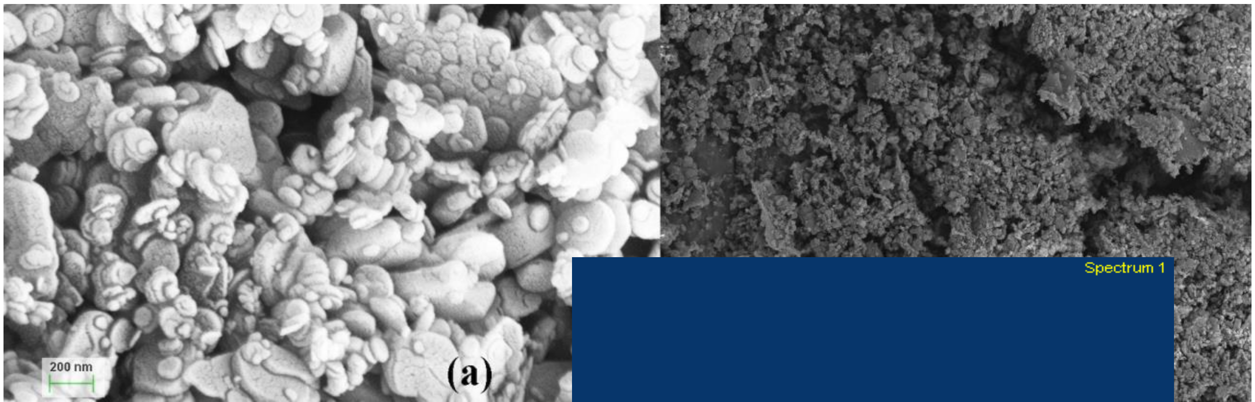

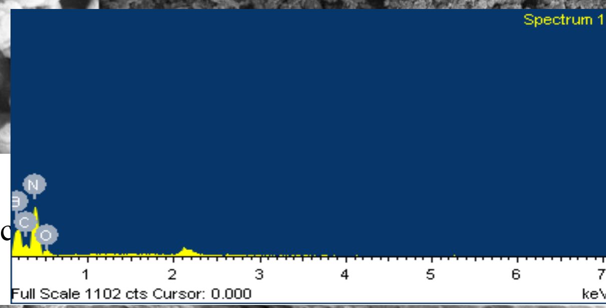

Fig. 3a. SEM mic

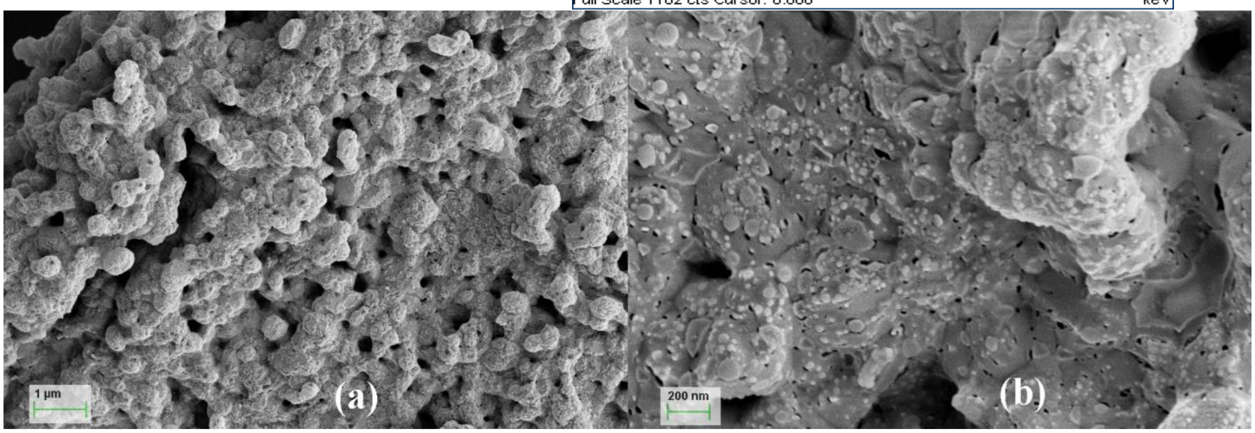

Fig. 3b. SEM micrographs of sulphur nanoparticles

EDAX spectra results clearly indicate that boron nitride consists of B (46.59 wt%), N (48.23 wt %), C (2.62 wt%), and O (2.56 wt%)and EDAX of sulphur results, where carbon and oxygen were originated from biomolecule moieties of the synthesized phytochemicals, S (82.27 wt%) and C (17.73 %) as shown in **Fig.** 4 (a) and **Fig.** 4(b).

Element	Weight %	Atomic%
B K	35.37	40.79
C K	14.06	14.60

N K	46.98	41.82
O K	3.59	2.80
Total	100.0	

Fig. 4(a) EDX spectra of Boron nitride.

Element	Weight%	Atomic%
C K	17.73	36.51
S K	82.27	63.49
Totals	100.00	

Fig. 4(b). EDX spectra Sulphur nanoparticles.

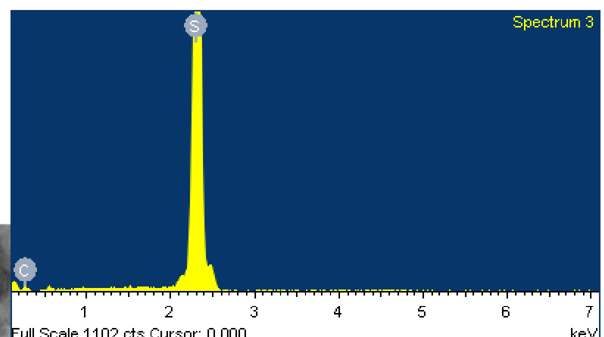

3.1.4 Transmission electron microscope

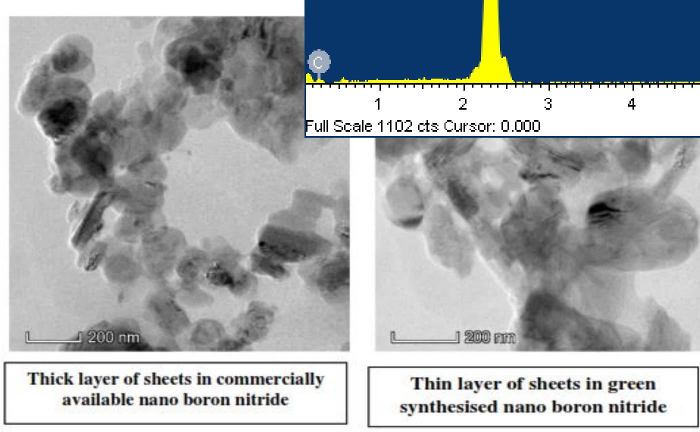

Fig. 5(a). TEM images of commercial and green synthesised nano boron nitride.

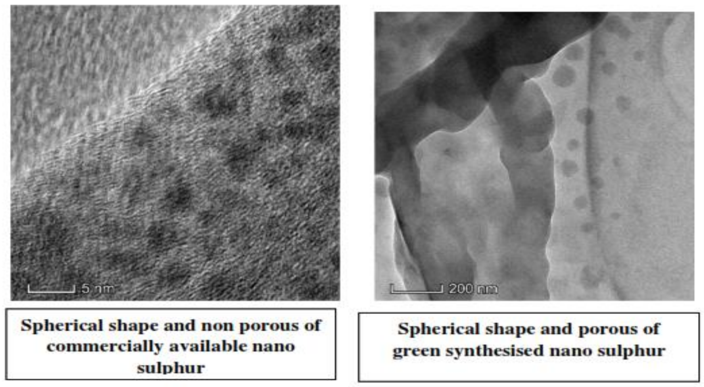

Fig. 5(b). TEM images of commercial and green synthesised nano sulphur.

The TEM morphology of the green-synthesized nano boron nitride was thin, transparent nano sheets with an average lateral dimension of 69 nm, as shown in **Fig.** 5(a). In case of boron nitride Commercially available boron nitride consists of a thick layer of sheets. The TEM images in **Fig. 5(b)** reveal that the commercially available nano sulphur was spherical and non porous (filled with inert carrier material), whereas the green-synthesized sulphur nano particle were spherical and porous. The pore size of the sulphur nanoparticles was in the range–8-12 nm. Whereas the ionic radius of the sulphate ion was 1.84 Å (1 Å = 0.1 nm), we can conclude that the morphology of the particles changed when they were converted into the nano-form. Porous particles are more efficient in penetrating plant tissue than nonporous particle because of their excellent accessibility to active sites and inherent controlled diffusion properties; hence, green synthesized nanoparticles are more efficient than commercially available nanoparticles.

3.1.5 Fourier Transformed Infrared spectroscopy

The FTIR spectra of green-synthesized boron nitride, as shown in **Fig. 6(a),** show two strong absorption bands located at 1385 and 810 cm^{-1} could be assigned to the in-plane B–N stretching vibration and out-of-plane B–N–B bending vibration, respectively. In addition, the peak centered at 3423 cm^{-1} can be attributed to the stretching mode of the -OH or H_2O groups. **Fig. 6(b)** shows the FTIR spectrum of sulphur nanoparticles with an intense peak at 2357 cm^{-1} corresponding to OCO bonds, and the peak at 3737 cm^{-1} is due to the external isolated –OH groups. The symmetric stretching vibration at 1396 cm^{-1} shows the presence of COO bonds. The peak at 3606 cm^{-1} shows the N–H stretching vibration. The shapes and positions of the peaks recorded for the green-synthesized particles were similar to those reported in the literature [Deane and Smith 2018].

3.1.6 UV-visible spectroscopy

A UV-visible spectrophotometer was used to confirm the presence of boron nitride and sulphur nanoparticle, as shown in **Fig. 6 (c)** and **(d).** Each element has its own spectral peak of absorbance; hence, by recording a particular peak value, we can determine the presence of a particular element. The results indicate that the main absorbance peaks of boron nitride nanoparticle were observed in the range of 250−258 nm. The peak at 252 nm indicated the successful formation of boron nitride nanoparticles, and the peak at 320 nm indicated the formation of sulphur nanoparticle. Similar results have been reported in [Bateni et al. 2019]. The Boron nitride shows Eg value of 2.4 eV and Sulphur nanoparticle shows the Eg value of 3.7 eV.

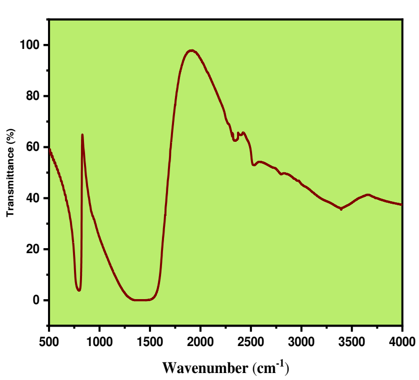

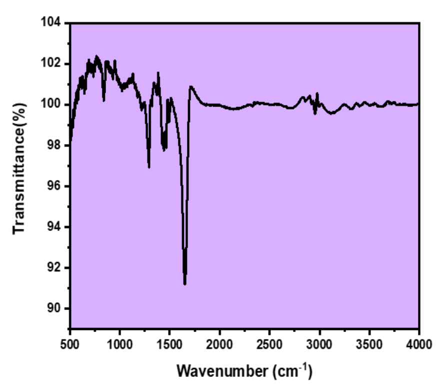

Fig. 6(a). FTIR spectra of nano boron nitride **Fig. 6(b).** FTIR spectra of nano sulphur.

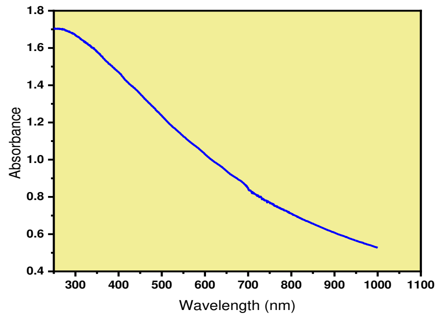

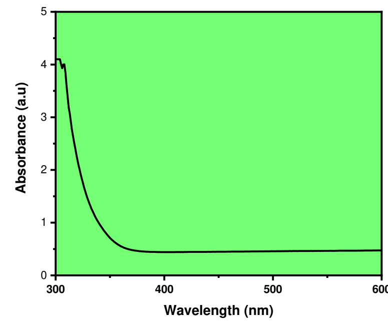

Fig. 6(c) UV-Visible absorbance of nano BN. **Fig. 6 (d)**. UV-Visible absorbance of nano S.

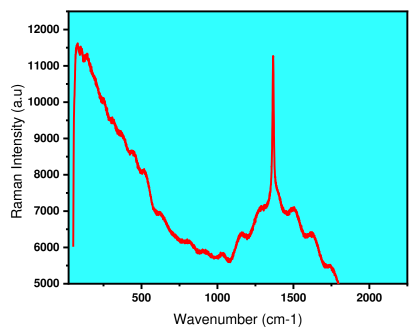

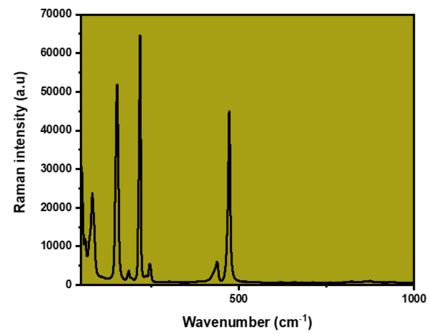

Fig. 6(e). Raman spectroscopy for nano boron nitride **Fig. 6(f)** Raman spectroscopy for nano sulphur.

3.1.7 Raman Spectroscopy

The Raman band for the green-synthesized nano boron nitride was observed at 1381 cm^{-1} which was attributed to the Raman active mode E_2g due to the in-plane atomic displacement of boron and nitrogen atoms against each other, as shown in **Fig. 6(e).** Raman peaks are associated with the lattice vibration and hence are affected by the atomic bond and chemical structure of the material. Thus, stress is present in the affected Raman peak. The crystalline structure and ordering of the hexagonal boron nitride layers were evaluated by Raman shift and full width at half maximum (FWHM) of the E_2g vibrational band. It is well known fact that High-quality single crystals (h-BN) exhibit an intrinsic E_2g vibration peak at 1367 cm^{-1}.

E_2g shifts to higher frequencies in polycrystalline materials. Domain size is also related to the FWHM of this peak, and fwhm increases with a decrease in size. In the present case, the blue-shifted E_2g vibration mode (1381 cm^{-1}) is due to the weaker interaction between the interlayer of boron nitride. The broadening of E_2g peak may be attributed to the shrinking size of the ordered boron nitride layers.

The Raman spectra of sulphur are shown in **Fig. 6 (f),** where the intensity of the line at 50 cm^{-1} corresponds to the fundamental component of the crystal vibrational symmetry. The Raman shifts for the line near 250 cm^{-1} were slightly different. This line corresponds to the S–S–S bonding because the shift for technical sulphur is lower (corresponding to lower energy). It can be stated that bending of long sulphur chains in technical sulphur occurs in less constrained conditions.

3.1.8 Particle size analysis

The sizes of the green-synthesized nano boron nitride and sulphur were analyzed using a particle-size analyzer. The size distribution of boron nitride analysis showed that 95 % of the particles were 82.74 nm in diameter (standard deviation 36.2 nm) and 5.3 % of the particles are 16.66 nm in diameter (standard deviation of 4.3 nm). The average size of the nano particle was 69.4 nm. The data clearly indicate that the particles are distributed homogeneously, as shown in **Fig.** 7(a), for boron nitride.

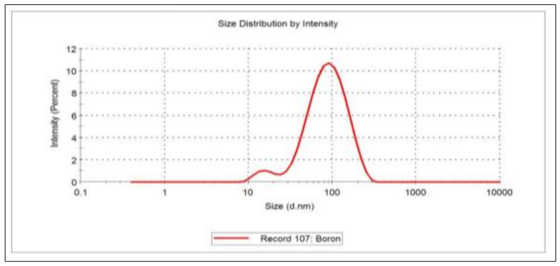

Fig. 7(a). Particle size distribution of nano boron nitride.

The size distribution of the sulphur analysis showed that 98 per cent of the particles were 70.74 nm in diameter (standard deviation of 39.2 nm) and 1.7 per cent of the particles were 56 nm in diameter (standard deviation of 1.2 nm). The average size of the sulphur nano particle is 60.2 nm. The data clearly indicate that the particles were homogeneously distributed. The PdI values <0.1 support the fact that the green-synthesized nano sulphur is monodispersed and there is almost no agglomeration, as shown in **Fig. 7(b).**

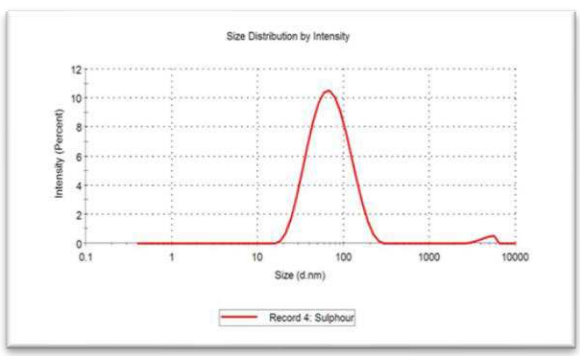

Fig. 7(b). Particle size distribution of nano sulphur.

3.2 *Laboratory studies: 2 sets of experiment were carried out to optimize the nano nutrient concentration for sunflower*

3.2.1 *Experiment I- Impact of nanoparticles on sunflower shoot growth and root characteristics*

In this research study, sunflower (*Helianthus annuus*) seeds were subjected to a series of treatments involving varying concentrations of chemically synthesized and green synthesized nano boron nitride, as well as nano Sulphur (**Fig. 8** and **Graph 1**). The concentrations tested included 250, 500, 750, 1000, 2000, and 3000 ppm. The primary objective was to assess the effects of these treatments on germination percentage, seedling vigor, and root morphology.

The results of the experiment revealed noteworthy findings. Notably, the treatment with 1000 ppm and 2000 ppm of green synthesized nano boron nitride led to significantly elevated germination percentages, improved seedling vigor, and the development of robust root morphology. However, in the case of chemically synthesized nano boron nitride, it was the 2000 ppm concentration that yielded the most favorable outcomes.

Interestingly, the application of nano Sulphur also produced distinct effects. Seedling vigor was notably enhanced when treated with 750 ppm concentrations of both green synthesized and chemically synthesized nano Sulphur.

Given these intriguing results, a subsequent series of experiments was undertaken. The purpose of this additional investigation was to refine the concentration ranges, further compare the performance of green synthesized and chemically synthesized nano particles, and ascertain their respective efficiencies. By conducting this comprehensive research, we aim to contribute to a deeper understanding of the potential benefits and variations in outcomes when utilizing different concentrations of chemically and green synthesized nano boron nitride and nano Sulphur. This research sheds light on the complex interplay between these treatments and sunflower seed development, ultimately paving the way for more informed and targeted agricultural practices.

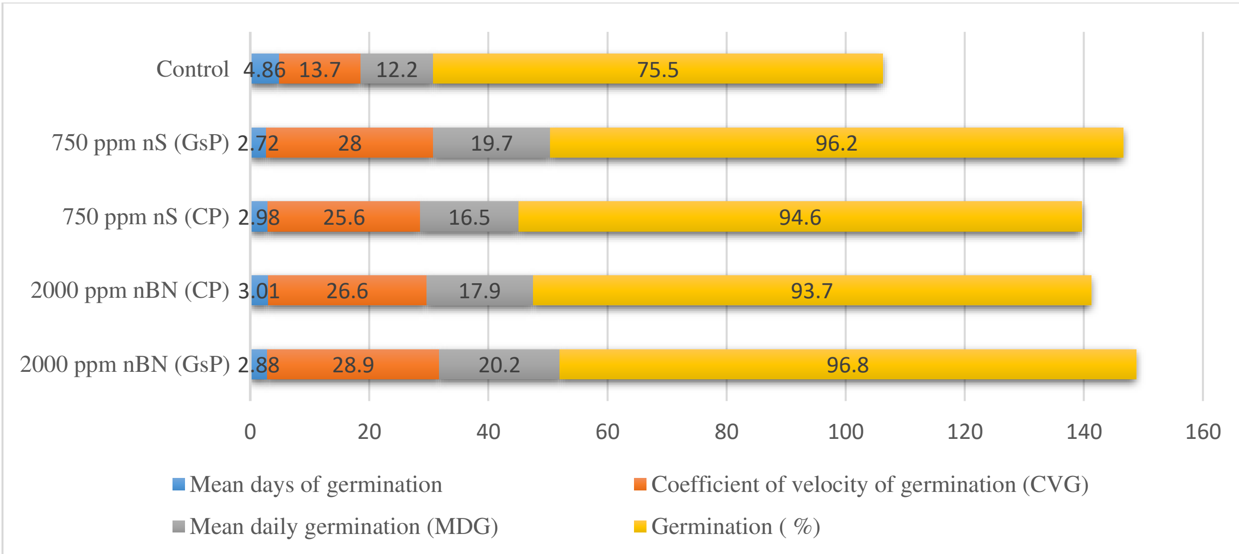

Graph 1: Impact of nanoparticles on sunflower germination parameters.

Fig. 8. Germination test with different forms and levels of nBN and nS. (Experiment-I)

3.2.2 Experiment II- Impact of nanoparticles on sunflower root and shoot morphology

The objective of this investigation was to refine the concentration levels employed in the experimental treatments. The detailed data corresponding to the growth parameters are explained and the visual representation is captured in **Fig. 9**.

Nano Sulphur treatments Nano boron nitride treatments

Fig. 9. Seedling vigour test with different forms and levels of nBN and nS (Exp -II).

3.2.2.1 Germination per cent, Mean days of germination (days), CVG and MDG

These treatments had a considerable effect on germination (Graph 2, 3(a) and 3(b). Germination was much greater (98.2%) in 1500 ppm nBN (GsP) compared to 600 ppm nS (GsP) (97.8%). Among the various concentrations of nBN (CP), the highest germination rate (93.8%) was observed at 2000 ppm. Among the several concentrations of nS (CP), the 750 ppm concentration had the highest germination rate (94.8%). The treatments had a considerable impact on the mean number of days of germination. The lower the mean number of days of germination, the faster is the seed germination. The control treatment had a significantly greater mean day of germination (4.98 days) than the other treatments. The lowest mean number of days of germination (2.19 days) was obtained in the 1500 ppm concentration of nBN (GsP). Among the various concentrations of nBN (CP), the 2000 ppm concentration had the lowest mean number of days of germination (2.98 days). Lower mean days of germination (2.44 days) were reported for different concentrations of nS (GsP), whereas lower mean days of germination (2.98 days) were recorded for different concentrations of nS (CP). These findings demonstrated considerable variation in the co-efficient of velocity of germination. The greater the CVG value, the faster the germination. CVG was significantly greater (32.9) in 1500 ppm nBN (GsP), which was comparable to that of 600 ppm nS (GsP) (32.4). Among the various concentrations of nBN (CP), the highest CVG value (27.1) was found at a concentration of 2000 ppm. Among the various concentrations of nS (CP), the highest CVG value (26.1) was found at 750 ppm. MDG (22.2) was significantly greater in 1500 ppm nBN (GsP) than in 600 ppm nS (GsP) (21.9). Among the various concentrations of nBN (CP), the 2000 ppm concentration had the highest MDG (18.1). Among the various nS (CP) concentrations, the 750 ppm concentration had the highest MDG (16.9) value.

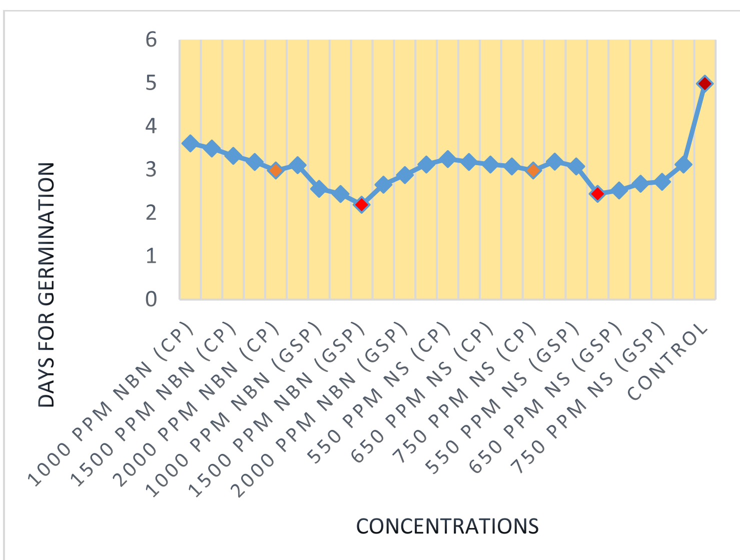

Graph 2. Mean days of germination of sunflower seeds.

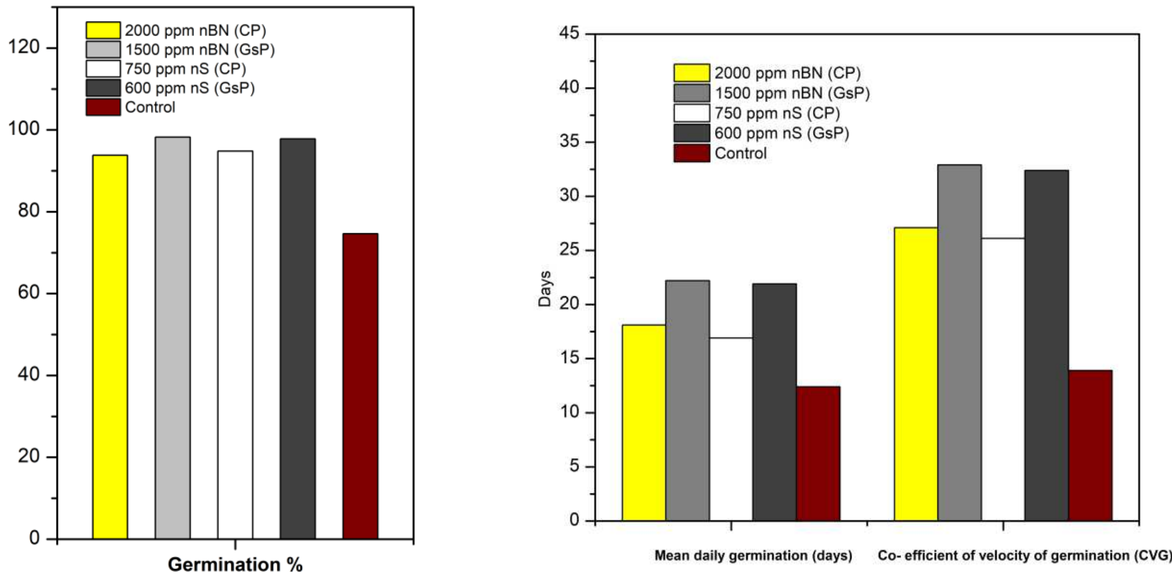

Graphs 3a & 3b. Germination%, MDG and CVG of seedlings.

3.2.2.2 Root and shoot length (cm)

The results showed that the various treatments had a substantial impact on root and shoot lengths (Graph 5) at 5 and 10 DAS. 1500 ppm nBN (GsP) resulted in significantly longer root length (10.98 and 19.81 cm at 5 and 10 DAS, respectively), comparable to that of 600 ppm nS (GsP) (10.87 and 19.42 cm at 5 and 10 DAS, respectively). The 2000 ppm concentration of nBN (CP) resulted in the longest root length (9.31 and 15.49 cm at 5 and 10 DAS, respectively). In contrast, the 750 ppm concentration of nS (CP) yielded the longest root length (8.89 and 16.43 cm at 5 and 10 DAS, respectively). Shoot length was significantly greater in 1500 ppm nBN (GsP) (12.99 and 18.29 cm at 5 and 10 DAS, respectively) than in 600 ppm nS (GsP) (12.89 and 18.24 cm at 5 and 10 DAS, respectively). The 2000 ppm concentration of nBN (CP) produced the longest shoot length (11.19 and 16.56 cm at 5 and 10 DAS, respectively). Among the various nS (CP) concentrations, the 750 ppm concentration produced the longest shoot length (10.81 and 16.21 cm at 5 and 10 DAS, respectively).

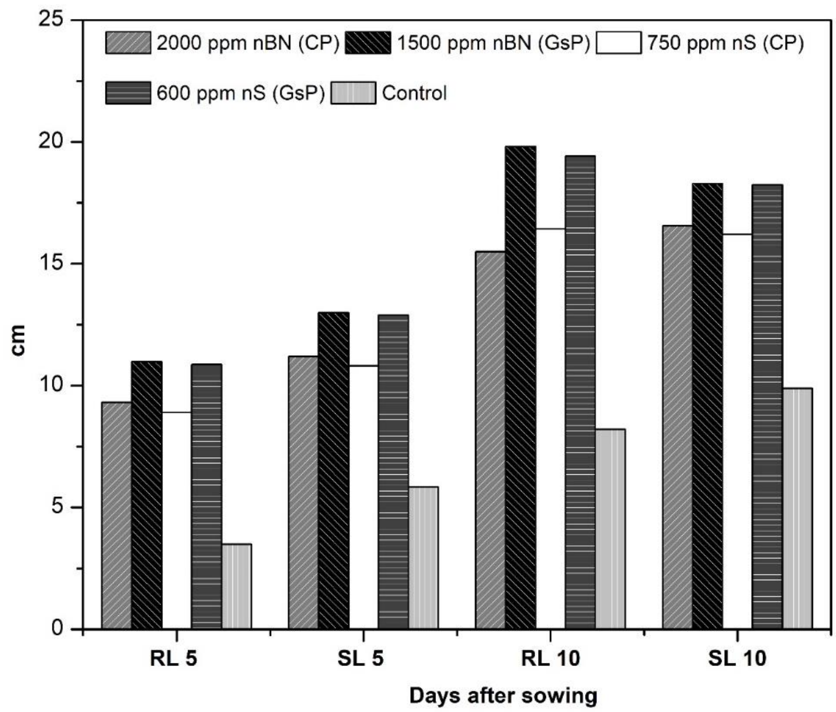

Graph 5. Root length (RL), Shoot length (SL) in cm at 5 and 10 days after sowing.

Nano boron nitride (GsP) concentrations above 1500 ppm and nano sulphur (GsP) concentrations above 600 ppm resulted in lower growth parameters, whereas nano boron nitride (CP) concentrations above 2000 ppm and nano sulphur (CP) concentrations above 750 ppm resulted in similar results in both sets of laboratory experiments. Higher growth parameters were reported in laboratory experiments using 1500 ppm nano boron nitride (GsP), 2000 ppm nano boron nitride (CP), 600 ppm nano sulphur (GsP), and 750 ppm nano sulphur (CP) (CP). When compared to commercially available nanoparticles, the quantity/concentration of nanoparticles (both nBN and nS) required to improve germination, shoot length, and root properties for the green-synthesized approach were lower.

Fig. 10(a). Root scanner images of sunflower seedlings as influenced by different forms and levels of 700 and 600 ppm nano sulphur application**.**

Fig. 10(b). Root scanner images of sunflower seedlings as influenced by different forms and levels of 1500 and 2000 ppm nano boron nitride application

3.2.2.3 Root parameters

The results showed that there was a significant difference with respect to root parameters (Graph 6 (a), 6 (b) 6 (c), 6 (d) 7 and **Fig.** 10 (a) and 10(b)) as influenced by different concentrations of green synthesized and commercial product of nBN and nS. Seed treatment with 1500 ppm nBN (GsP) recorded higher average root diameter (1.35 mm), root volume (1.81 cm^3), root length volume (109989 cm m^3), surface area (70.89 cm^2) and forks (4887) which was on par with 600 ppm of nS (GsP). Seed treatment with 600 ppm of nS (GsP) recorded average root diameter (1.32 mm), root volume (1.76 cm^3), root length volume (109796 cm m^3), surface area (70.86 cm^2) and forks (4865). Among different levels of nBN (CP) higher average root diameter (0.63 mm), root volume (1.04 cm^3), root length volume (97246 cm m^3), surface area (67.89 cm^2) and forks (4244) was recorded in 2000 ppm concentration. Among different levels of nS (CP) higher average root diameter (0.91 mm), root volume (1.35 cm^3), root length volume (85431 cm m^3), surface area (67.89 cm^2) and forks (4333) was recorded in 750 ppm concentration.

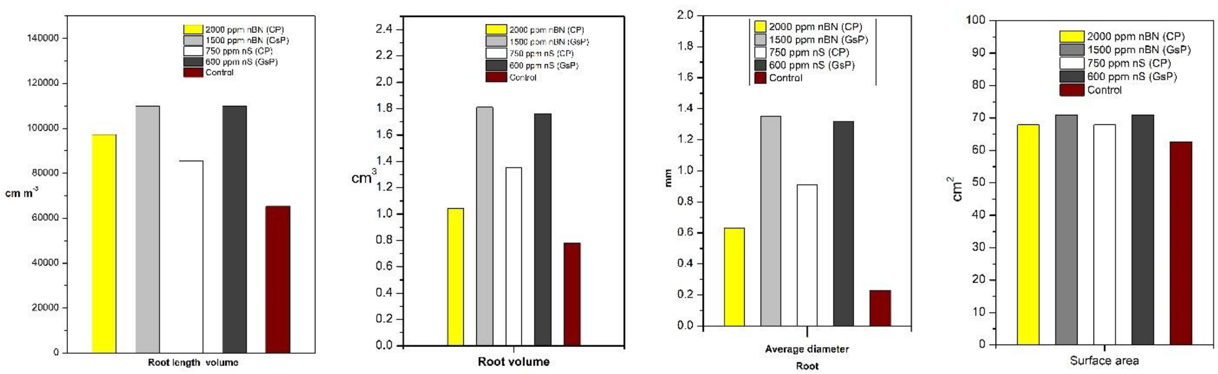

6 (a) 6 (b) 6(c) 6(d)

Graph 6 (a), 6 (b), 6 (c) and 6 (d). Root characteristics of sunflower seedlings, as influenced by different nanoparticles.

An increase in the concentration of nBN (GsP) over 1500 ppm and nS (GsP) over 600 ppm recorded lesser growth parameters but nBN (CP) 2000 ppm and nS (CP) 750 ppm recorded similar results in both sets of laboratory experiments. According to the results recorded in the laboratory experiment, higher growth parameters were recorded by 1500 ppm nBN (GsP), 2000 ppm nBN (CP), 600 ppm of nS (GsP) and 750 ppm of nS (CP).

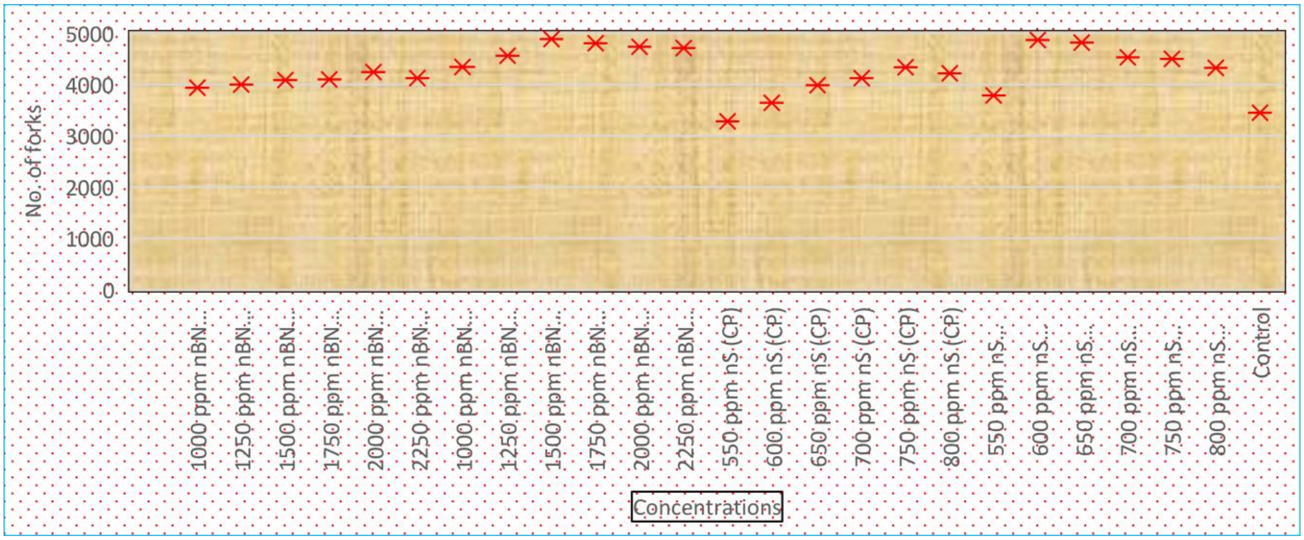

Graph 7. Number of forks in roots of sunflower as influenced by different concentrations of Nanoparticles.

Discussion

4.1 Effect of nanoparticles on Germination, Mean days of germination (days), CVG, MDG of sunflower seeds.

Compared to the control, seed treatments with nBN and nS had higher coefficients of velocity of germination, mean daily germination, and reduced mean days of germination. Higher CVG, MDG and lower mean days of germination indicated that the seeds germinated well. The mean number of days required for cotton germination was reduced by 50% in plots treated with nano boron nitride [Pruthviraj and Chandrashekara 2019]. When nanoparticles are seeded, they enter the cell via plasma membrane invagination via vesicles that can migrate to different compartments of the cell [Konate et al. 2018]. Using X-ray computed nanotomography and hyperspectral imaging microscopy, Du et al. 2018 discovered that Arabidopsis thaliana seedlings treated with nanoparticles exude mucilage, which enhances germination by a factor of ten. Maurizio et al. 2014 investigated the effect of four metal oxide nanoparticles on watermelon crop peak value and germination value. Using transmission electron microscopy, they discovered that tiny nanoparticles could pierce watermelon seeds and enter the epicotyl area. [Konate et al. 2018] evaluated the germination value of cucumber seeds treated with CeO_2 nanoparticles and discovered an increased coefficient of velocity of germination in nano CeO_2 seed treatment compared with regular CeO_2 seed treatment. According to Kallol et al. 2014, nanoparticles boost amylase activity in oilseed crops and promote germination under stressful conditions. Singh et al. 2016 observed greater germination percentages in tomato seeds and stated that tomato seed germination took 22 h less than that of untreated seeds. Dhage and Patil 20018 found that when maize seeds were treated with nano sulphur, they had a greater peak value and germination value, and that the higher the peak value, the faster the seeds germinated under stressful conditions. Sunflower exhibit leaf adaptive mechanisms to overcome nutrient and water-stressed conditions for effective germination [Ouvrard et al. 1996]. The research findings showcased the intricate regulation of certain low molecular weight (LMW) heat shock proteins (HSPs) within the plant's cytoplasm, indicating their potential role in sunflower growth by enhancing water and nutrient stress tolerance [Coca et al. 1994]

4.2 Effect of nanoparticles on shoot and root growth, SVI-I and II in sunflower seeds.

When compared to untreated seeds, nano boron nitride- and sulphur-treated seeds reported higher shoot development, root growth, and seedling vigor. The enzymatic activity of seeds for germination increases if they are treated with fine particulate matter, such as nano. Under salt water treatment, *Jussiaea rapens* primed with nano Zinc oxide showed increased root and shoot development, as well as increased synthesis of carbonic anhydrase to counteract the negative effects of excess salts, but conventional ZnO-treated plants produced relatively little [Wenhui et al. 2012]. When seeds are exposed to nanoparticles, they react differently to normal-sized particles, this was observed using a scanning electron microscope of sunflower seeds [Prasad et al. 2012]. Seedling vigor was improved by 21% when sunflower seeds were primed with nano ZnO under stressful conditions compared to untreated seeds. This may be attributed to the quicker transportation of nanoparticles into the tissue, stimulating cells for higher cell multiplication [Faten et al. 2018]. According to Hemantharanjan et al. 2018 seed priming with nano sulphur (800 ppm) increased root and shoot development in tomato seedlings and increased SVI-I (1915) in tomato seedlings. Suleiman et al. 2015 found that seed priming with nano boron nitride (500 ppm) increased shoot and root development in niger seeds by increasing amylase and cellulase enzyme production. They also found greater SVI-I and SVI-II in the same treatment group than in the control group. Nano iron particles reduced the oxidative stress in photosynthetic apparatus by non-enzymatic and enzymatic antioxidant activity. It resulted in increased total chlorophyll content and plant biomass [Aarti et al. 2019]. Plants utilize complex mechanisms to acquire minerals from the rhizosphere, transport them from roots to shoots, and deliver them to developing tissues and edible parts of the plants. Uptake of these metals is extremely complex and tightly regulated [Khurram et al. 2019].

4.3 Effect of nanoparticles on root parameters of sunflower seeds

The results revealed a considerable variation in root characteristics impacted by various quantities of green-synthesized and commercial nano boron nitride and sulphur seed priming. Seed treatments with 1500 ppm nano boron nitride (GsP) and 600 ppm nano sulphur (GsP) resulted in longer root length, larger root volume, surface area, and forks (root parts responsible for water and nutrient absorption). If the root parameters have a greater value, the roots grow quicker and absorb more water and nutrients from the soil, which is necessary in dryland settings. These findings are consistent with those of [Pruthviraj and Chandrashekara 2021 b], who found that root volume was increased in ZnO-treated plots compared with control treatment. Geetha et al. observed increased root development when sunflower seeds were treated with nano boron nitride and found that seed treatment with nano sulphur (420 ppm) resulted in longer root length (389 cm) and larger root volume (1.25 cm^3) in the sunflower crop than in the control.

Pruthviraj and Chandrashekara (2019) discovered an increased nutrient transfer to forks in roots during the early phases of root growth, suggesting that seed treatment with nutrients promotes root growth over the control. Enhanced root volume and root diameter were observed in sunflower seedlings treated with nano boron nitride (600 ppm), which is responsible for plants overcoming transplanting shock. Nano boron nitride (GsP) concentrations above 1500 ppm and nano sulphur (GsP) concentrations above 600 ppm resulted in lower growth parameters, whereas nano boron nitride (CP) concentrations above 2000 ppm and nano sulphur (CP) concentrations above 750 ppm resulted in similar results in both sets of laboratory experiments. Higher growth parameters were reported in laboratory experiments using 1500 ppm nano boron nitride (GsP), 2000 ppm nano boron nitride (CP), 600 ppm nano sulphur (GsP), and 750 ppm nano sulphur (CP).

4.4 Root parameters

The findings identified a significant variation in root characteristics as impacted by various concentrations of a green-synthesized and commercial product of nBN and nS. Seed treatment with 1500 ppm nBN (GsP) resulted in a larger average root diameter (1.35 mm), root volume (1.81 cm^3), root length volume (109989 cm m^3), surface area (70.89 cm^2), and forks (4887) than 600 ppm nS. (GsP). The average root diameter (1.32 mm), root volume (1.76 cm^3), root length volume (109796 cm m^3), surface area (70.86 cm^2), and forks were measured after seed treatment with 600 ppm of nS (GsP) (4865). Increases in nBN (GsP) concentrations above 1500 ppm and nS (GsP) concentrations above 600 ppm resulted in lower growth parameters, although nBN (CP) 2000 ppm and nS (CP) 750 ppm yielded identical findings in both sets of laboratory studies. According to the laboratory experimental results, increased growth parameters were recorded for 1500 ppm nBN (GsP) and 600 ppm nS (GsP). Enhanced root growth and root growth parameters were observed in cotton seedlings when treated with nano zinc (Pruthviraj and Chandrashekara 2021a)

5. Conclusions

Nano boron nitride and sulphur were prepared via an eco-friendly green synthesis method using different plant extracts. To synthesize nano boron nitride, *Cassia fistula* leaf extractant was used, similar to the synthesis of nano Sulphur, *Simarouba glauca* leaf extractant. After obtaining green-synthesized nano boron nitride, sulphur particles were characterized using different instruments. PXRD was used to determine the purity of the prepared samples. The UV–Vis spectrophotometer indicated that the main absorbance peaks of the nano particle were observed in the range of 250–258 nm. Similarly, for sulphur, the main absorbance peaks were observed in the range of 260-285 nm. The average size of boron nitride nano particle was 69.4 nm and that of sulphur nano particle was 60.2 nm. TEM showed that commercially available nano sulphur was spherical in shape and non-porous (filled with inert carrier material), whereas the green-synthesized sulphur nanoparticle were spherical and porous. In the case of boron nitride commercially available boron nitride contains a thick layer of sheets, which are green-synthesized nano boron nitride thin, transparent nanosheets with an average lateral dimension of 69 nm. For seed treatment, nano fertilizers must be optimized because the excessive application may block cells and lower metabolic activity. Compared to green-synthesized nanoparticles, commercially available nano fertilisers are less effective in promoting seed germination and crop growth. Greenly synthesized nanoparticles are more effective than conventional fertilizers and are environmentally friendly. Sunflower seed germination was improved by the synergistic interaction between sulphur and nano boron nitride. This method can be used in dry lands where there is a lack of nutrients and water to generate larger economic returns.

Declaration of Competing Interest

The authors declare no conflict of interest associated with this manuscript.

References

1. Aarti RD, Ji WJ, Su JL, Go UP, Beom SK (2019) Ultrasound-Assisted facile green synthesis of hexagonal boron nitride nanosheets and their applications. ACS Sust Chem Eng 7:17114−17125.
2. AnilKumar GN, Shruthi DL (2021) The nature of the chemical bond in sodium tungstate based on ab initio, DFT and QTAIM topological analysis of electron density. Materials Today Proc 44: 3127-3132.
3. Anonymous (2011) International seed testing association. Seed Sci Tech 5(2): 56-89.
4. Awwad AM, Salem NM, Abdeen AO (2015) Novel approaches for synthesis of sulphur (S-NPs) nanoparticles using *Albizia julibrissin* fruits extract. Adv Materials Letters 6: 432-435.
5. Bateni A, Erdem E, Habler W, Somer M (2019) High-quality MgB_2 nanocrystals synthesized by using modified amorphous nano-boron powders: Study of defect structures and super conductivity properties. AIP Advances 9(4): 1-7.
6. Chaudhari RG, Paria SJ (2010) Synthesis of sulphur nanoparticles in aqueous surfactant solutions J Colloid Interface Sci 343: 439-446.
7. Chen D, Huang Y, Hu X, Li R, Qian Y, Li D (2018) Green synthesis of boron carbonitride with high capacitance. Materials 11(387): 1-7.

8. Chitdeshwari T, Poongothai S (2003) Yield of groundnut and its nutrient uptake as influenced by zinc, boron and sulphur. Agri Sci Digest 23(4): 263-266.
9. Coca MA, Almoguera C, Jordano J (1994) Expression of sunflower low-molecular-weight heat-shock proteins during embryogenesis and persistence after germination: localization and possible functional implications. Plant Mol Biol 25:479–492. https://doi.org/10.1007/BF00043876
10. Deane K, Smith RJ (2018) Joint commission on powder diffraction standards powder diffraction file, inorganic phase International center for diffraction data. PA, USA. JCPDS 08247: 410.
11. Dhage SJ, Patil PA (2008) Effect of sulphur sources and their rates on yield, growth parameters, uptake of nutrients and quality of sunflower. Asian J. Soil Sci 3(2): 323 - 325.
12. Dongping C, Yanzhen H, Xinling H, Rongkai L, Yingjiang Q, Dongxu L (2018) Green synthesis of boron carbonitride with high capacitance. Materials 11:387. doi:10.3390/ma11030387
13. Du W, Tan W, Yin Y, Ji R, Guo H, Gardeatorresday JL (2018) Different effects of copper nanoparticles/microparticles in agronomic and physiological parameters of oregano (*Origanum vulgare*.). Sci Total Environ 618: 306-312.
14. Edwards K, Chandrashekhara S, Suresh B, Singh R, Kavitha S (1932) Effect of planting geometry on yield and yield attributes of bajra. J Agron 1(2):19-33.
15. El-Bialybe, Ragaa A, Khaled SH, Hamza HA (2017) Cytotoxic effect of biosynthesized silver nanoparticles on ehrlich ascites tumor cells in mice. Int J Pharmacology 13: 134-144.
16. Faten Z, Mustafa H, Muayad A (2018) Synthesis of nano sulphur particles and their antitumor activity. J Microbiol Biochemical Tech 10(3):59-68.

17. Geetha KN, Kavita MG, Lingaraju NN, Ramesh R, Shankar AG, (2018) Seed priming with nano boron nitride increases the performance of Sunflower (*Helianthus annuus* L.) seedlings. Int J Current Microbiol Appl Sci 7:503-508.

18. Hemantharanjan A, Trivedi AK, Maniram K (2018) Effect of foliar applied nanoboron and soil applied iron and sulphur on growth and yield of soybean (*Glycine max* L. Merr). Indian J Plant Physiol 5: 141-144

19. Joshi S, Joshi S (2002) A book on oil tree- *Laxmitaru glauca*, University of Agricultural sciences, Bangalore and Indian council of Agricultural Research, New Delhi, India.

20. Kallol B, Jajati M, Hirak B, Ayon A, Krishnendu R, Amit P (2014) Nano boron fertilization in sunflower (*Helianthus annuus* L.) in an *Inceptisol* of West Bengal. Comm Soil Sci Plant Anal 46(4): 528-544.

21. Kasra M, Hosseein AF, Omid M (2011) Evaluation of nano priming on germination percentage in green gram (Vigna radiata L.) Adv in Environ Bio 5(11): 3659-3663.

22. Khairan K, Zahraturriaz, Jalil Z (2019) Green synthesis of sulphur nanoparticles using aqueous garlic extract (*Allium sativum*). Rasayan J Chem 12(1): 50–57.

23. Khurram B, Motoaki S, Naoko KN, The transport of essential micronutrients in rice. Molecular Breed 39:168. https://doi.org/10.1007/s11032-019-1077-1

24. Konate A, Wang Y, He X, Adeel M, Zhang P, Ma Y, Ding Y, Zhang J Y, Ang J, Kizito S, Rui Y (2018) Comparative effects of nano and bulk-Fe_3O_4 on the growth of cucumber (*Cucumis sativus*.). Ecotoxicol & Environ Safety 165: 547-554.

25. Kouzegaran VJ, Farhadi K (2017) Green synthesis of sulphur nanoparticles assisted by a herbal surfactant in aqueous solutions. Micro & Nano Letters 12(5): 329-334.

26. Li M, Zhang L J, Tao L, Li W (2008) Ecophysiological responses of *Jussiaea rapens* to cadmium exposure. Aquatic Botany 88: 347-352.

27. Maiti SK, Giri G, (2003) Influence of phosphorus and sulphur fertilization on productivity and oil yield of groundnut (*Arachis hypogae*) and sunflower (*Helianthus annuus*) in intercropping with simultaneous and staggered planting. Indian J Agron 48(4): 267-270.

28. Marschner H, Romheld V, Kissel M (1986) Different strategies in higher plants in mobilization and uptake of iron. J Plant Nutr 9: 695-713.

29. Maryam, Mazaheri-Tirami, Ashraf K, Mehrana KD (2022) The role of iron nanoparticles on morpho-physiological traits and genes expression (IRT_1 and CAT) in rue (*Ruta graveolens*). Plant Mol Biol 110:147–160.

30. Maurizio V, Gianmarco B, Davide M, Davide N, Cristina B, Antonio SS (2014) Nano-sized boron synthesis process towards the large scale production. Chemical Eng J 256:32–38.

31. Medina-Parez G, Fernandez-Luqueno F, Trejo-Tellez LI, Pampillon-Gonzalez L (2018) Growth and development of common bean *(phaselous vulgaris* L.*)* exposed to iron, titanium and zinc oxide nanoparticles in an agricultural soil. Appl Eco Environ Res 16(2): 1883-1897.

32. Nida MS, Luma SA, Akl MA (2016) Green synthesis of sulphur nanoparticles using *Punica granatum* peels and the effects on the growth of tomato by foliar spray applications. Environ Nanotech Monitoring & Manag 6: 83‑87.

33. Ouvrard O, Cellier F, Ferrare K (1996) Identification and expression of water stress- and abscisic acid-regulated genes in a drought-tolerant sunflower genotype. Plant Mol Biol 31: 819–829. https://doi.org/10.1007/BF00019469

34. Prasad TN, Sudhakar P, Sreenivasulu Y, Latha P, Munaswamy V, Rajareddy K, Sreeprasad T S, Sajanlal PR, Pradeep T (2012) Effect of nanoscale boron particles on the germination, growth and yield of peanut. J Plant Nutri (35): 905-927.

35. Pruthviraj N, Chandrashekara CP (2019) Nano zinc seed treatment and foliar application on growth, yield and economics of Bt Cotton (*Gossypium hirsutum* L.). Int J Curr Microbiol App Sci 8(8): 1624-1630.

36. Pruthviraj N, Chandrashekara CP (2021a) Impact of nano zinc oxide application on quality parameters of Bt cotton (*Gossypium hirsutum* L.). Int J Chemical Studies 9(2): 153-158. https://doi.org/10.22271/chemi.2021.v9.i2b.11939.

37. Pruthviraj N, Chandrashekara CP (2021b) Soil and plant nutrient status of cotton as influenced by different methods of application of nano ZnO. J Pharmacognosy Phytochem 10(2): 1386-1389. https://doi.org/10.22271/phyto.2021.v10.i2r.14011.

38. Rahimi A, Bussler W, (1973) The effect of copper deficiency on the tissue structure of higher plants. Z Pflanzenerachr 135: 183-195.

39. Russell PE, Mussa AEA (1977) An evaluation of potential seed treatments to control *Fusarium solani*, the cause of foot and root rot of *Phaseolus vulgaris*. J Agric Sci 89: 235–238.

40. Shruthi DL, A Jagannatha R, GN Anil K, CK Jayasankar (2020) Judd ofelt theoretical analysis, Photoluminescence properties of Eu_3+activated LiGd(WO_4)2 phosphors. J of Luminescence 222:117-167.

41. Singh B, Kaur G, Singh P (2016) Nanostructured boron nitride with high water dispersibility for boron neutron capture therapy. Sci. Rep 6: 35535.

42. Suleiman M, Al-Masri M, Ali AA, Aref D, Hussein A, Saadeddin I, Warad I (2015) Synthesis of nano-sized sulphur nanoparticles and their antibacterial activities. J of Materials and Environ Sci 6(2): 513-518.

43. Suresh D, Nethravathi P C, Udayabhanu H, Rajanaika H, Nagabhushana H, Sharma S C (2015) Green synthesis of multifunctional zinc oxide (ZnO) nanoparticles using *Cassia fistula* plant extract and their photo degradative, antioxidant and anti-bacterial activities. Mater. Sci. Semiconductor Processing 31: 446-454.

44. Wanga Y, Han J, Li Y, Chen H (2018) Progress in preparation, properties and application of boron nitride nanomaterials. AIP Conference Proc 1864:020132: 1-5.

45. Wenhui Y, Yejian G, Li L (2012) Green synthesis of graphene/Ag nanocomposites. App Surface Sci 261: 753-758.

46. Weon G S, Steven C, Ozan U, Steven L G (2011) Production and characterization of boron nanoparticles synthesized with a thermal plasma system. J Nanoparticle Res 13:7187–7191.

Supplementary Files

This is a list of supplementary files associated with this preprint. Click to download.

- AuthorContributationStatement.docx
- Supplementarymaterial.docx